Modulation of the phenotypic and functional properties of phagocytic macrophages by wear particles from orthopaedic implants

N. AL-SAFFAR*, P. A. REVELL, A. KOBAYASHI
Department of Histopathology, and The Interdisciplinary Research Centre In Biomedical Materials, London, Royal Free Hospital School of Medicine, Hampstead, London NW3 2PF, UK

An attempt was made to assess the local chronic inflammatory response in patients with failed orthopaedic implant that is clinically associated with osteolysis, bone and bone marrow necrosis. The main objective was to analyse the heterogeneity of the macrophage functional subsets in the bone–implant interface membrane and to evaluate their possible role in the development of an erosive inflammatory lesion within the bone. Immunohistology was performed on 21 specimens of the bone–implant interface obtained from 17 patients during revision arthroplasty, and synovial membranes from rheumatoid (RA, $n = 4$), and osteoarthritis (OA, $n = 4$) patients. Three well-characterized monoclonal antibodies (MAb) recognizing antigenic determinants on specific functional subsets of macrophages (Mϕ) were used. RFD1 (interdigitating reticulum cells/antigen presenting cells, (APC), RFD7 (mature phagocytic macrophages), and RFD9 epithelioid cells and foreign body giant cells (FBGC). RFD1 was expressed on a variable number of perivascular and synovial lining Mϕ in both RA and OA synovia, at a frequency of 25%–40%. In cases with total joint replacements, the interface showed a marked increase in the expression of RFD1 (20%–90%). A considerably greater percentage of RFD1 positive Mϕ and FBGC was noted in the interfaces from cases with a high level of detectable metal particulate wear debris (mean 80%, range 60%–90%) than in cases with polyethylene wear debris (mean 30%, range 0%–50%), p 0.0001. RFD7 labelled most tissue Mϕ in each group. Immunoreactivity for RFD9 was restricted to FBGC in all cases analysed. The finding of elevated expression of RFD1 on metal-containing Mϕ and FBGC in the bone-implant interface suggests an increase in antigen-presenting phenotype and indicates that metal particles have more impact in the induction of immune-mediated responses. Such responses are characterized by sustained cellular hyperreactivity and phenotypic changes in Mϕ subsets.

1. Introduction

The cellular response to particulate material from orthopaedic implants is well documented. Such particles are generated during wear at the articulation or by micromotion between different implant components and the bone [1]. Increased levels of metal or polyethylene (PE) particles have been demonstrated locally within the synovial tissue, bone trabeculae and bone marrow [2], as well as in the serum and urine of patients with total joint replacements (TJR) [3, 4]. Recent reports described dissemination of these particles to regional lymph nodes, liver and spleen [5–7]. Various immunopathological changes have been shown to be induced by wear particles released from orthopaedic implants. These include chronic inflammation within the joint that is associated with a foreign-body granulomatous response [8]. Inflammatory Mϕ and giant cells within these lesions act directly on adjacent bone surfaces, leading to focal osteolysis/bone resorption and the clinical failure of TJR [9, 10]. Various studies have also demonstrated bone and bone marrow necrosis, lymphadenopathy with sinus histiocytosis and the formation of tumours in association with particulate wear debris [7, 11–13]. Recently a case of granulomatous hepatitis associated with epithelioid histiocytes, lymphocytes and multinucleated giant cells has been reported [14].

The present study focused on the potential role of released particulate material in the cellular transformation around the prosthetic joint. The phagocytosis of such indigestible particles by local macrophages (Mϕ) and the persistent exposure of

* Author to whom all correspondence should be addressed.

0957–4530

these cells to such an antigenic stimulus, results in the accumulation of Mϕ subsets within the fibrous tissue found at the bone–implant interface [10]. Histological assessment of the interface membranes indicates that Mϕ are the most abundant cells in these tissues. The chronic inflammatory response is characterized by the appearance of different forms of Mϕ, including histiocytic, dendritic and stellate Mϕ and the formation of foreign body giant cells (FBGC) [15].

Little is known about the phenotypic and functional diversity of the Mϕ subsets in the bone-implant interface membranes. Similarly, there has been no previous work investigating the contribution of various types of implant derived particulate material in promoting the migration and differentiation of specific functional subsets of Mϕ and the formation of histologically distinct erosive lesions next to the bone. The study highlights the potential antigenicity of metallic particulate wear debris. It also demonstrates that the release of metal debris from orthopaedic prostheses can significantly increase the proportion of antigen presenting macrophages within the joint which may augment the cellular response leading to persistent local chronic inflammatory reactions.

2. Materials and methods

2.1. Patients and controls

A total of 21 specimens of the bone–implant interface was obtained from 17 patients during revision of aseptically loosened hip ($n = 10$) or knee ($n = 7$) arthroplasties. The initial diagnosis that led to joint replacement was rheumatoid arthritis (RA) ($n = 6$), and osteoarthritis, (OA) ($n = 11$). Revision of TJR in these patients was performed for aseptic loosening that showed associated bone resorption at variable locations and severity in radiographs. No microorganisms were grown from the tissues in any of the cases using standard microbiological methods. Brief clinical details of the patients studied are summarized in Table I.

In addition to the interface tissue samples, fresh synovial membranes obtained during total knee replacement from patients with RA ($n = 4$), and OA ($n = 4$) were included in the study. One synovium with normal histology obtained during amputation was also used as a control.

2.2. Tissue processing and preparation

Tissue samples collected were covered in OCT mounting medium, snap frozen in liquid nitrogen-cooled isopentane, and stored at $-70\,^{\circ}C$ until use. A small piece of each sample was taken before freezing and used for histological examination. These were fixed in buffered formol saline for at least 48 h and processed to paraffin wax. Paraffin and frozen sections, 5 μm thick were stained with haematoxylin and eosin in order to define clearly the cellular morphology.

2.3. Antibodies

Three monoclonal antibodies (MAb), RFD1, RFD7 and RFD9 were used for the characterization of Mϕ functional subsets in the tissue samples studied. The MAb were a gift from the Department of Clinical Immunology, Royal Free Hospital School of Medicine, London. The specificity of the antibodies, their reactivity with various Mϕ populations and the

TABLE I List of patients studied and their clinical data

Case No.	Sex/Age	Joint involved/ revision no/ interface tissue	Clinical findings before and during revision[a]
1.	M/57	Hip/1/A	Inflammatory arthropathy 10 y. Developed osteoarthritic changes 7 y ago
2.	M/78	Hip/1/A,F	Mild RA. Marked acetabular bone loss. Clinical evidence of loosening of both components confirmed by X-ray
3.	M/40	Hip/2/F	Both components were loose due to bone resorption
4.	M/66	Knee/1/F,T	Remarkable bone lysis around the tibial component stem. Thick granulation tissue removed. Large amount of PE and metal debris. Bilateral TKR, both revised within 1 y
5.	F/63	Knee/1/T	25 y history of RA. Five TJR in the last 16 y, 1 previous revision
6.	F/34	Hip/2/A,F	Severe osteolysis at several points on acetabulum. Required bone grafting. Five TJR in the last 17 y, and 4 previous revisions on different joints
7.	F/54	Hip/1/A	Acetabulum and previous bone graft were severely eroded and fractured. Large amount of PE around tissue and bone. Bilateral THR
8.	F/60	Hip/1/A,F	Bone erosion on the femoral side. Femoral canal was eroded and required grafting
9.	F/46	Hip/1/F	Gross loosening of acetabular component due to bone erosion. Graft to acetabulum during revision. Femoral proximal resorption
10.	F/77	Knee/2/T	Revised due to pain and loosening, also inflamed synovium
11.	F/85	Hip/1/F	Bone erosion of femur
12.	M/56	Hip/1/F	Femoral bone loss at the proximal side
13.	M/46	Knee/1/T	Trabecular bone loss and bone atrophy that did not show on the X-ray
14.	M/76	Knee/1/F	Radiographic evidence of bone lysis on the femoral and tibial side, and bone necrosis
15.	M/50	Hip/2/F	Osteolysis on the femoral side only. Required bone grafting
16.	M/58	Knee/1/T	Radiolucent lines around tibial component
17.	F/65	Knee/1/T	Revision for patellar dislocation. Bilateral TKR for OA

[a] PE, polyethylene; TKR, total knee replacement; THR, total hip replacement; A, acetabular Interface; f, Femoral interface; t, tibial interface.

staining pattern in other tissues have been previously assessed and described [16, 17]. RFD1 is an IgM MAb that recognizes a 28–33 KD epitope within the class II HLA-DR molecule, and shows immunoreactivity with interdigitating reticulum cells (ID) in the T cell areas of peripheral lymphoid tissues, as well as in the thymic medulla. It does not label tissue macrophages, Kupffer cells or Langerhans cells. RFD7 is an IgG_1 MAb that precipitates a 77KD antigen which has a broad tissue distribution. It reacts with tissue Mϕ/histiocytes in the marginal zone of the lymphoid tissue as well as most alveolar and peritoneal Mϕ. It also labels cells in the thymic cortex and Kupffer cells. It does not react with Langerhans cells or tingible body macrophages [18]. Finally, RFD9 was found to react specifically with tingible body Mϕ in the lymphoid follicles, epithelioid Mϕ and foreign body giant cells in granulomas [19].

Other antibodies used in this study were: rabbit antibody to IL-1β which reacts with IL-1β precursor and secreted forms (Genzyme); MAb to macrophage associated antigens CD68 (EBM11), CR3 (CD11b, CD18) and aminopeptidase-N (CD13), all from Dako. Finally anti CD3 MAb (Dako) was used to identify T cells.

2.4. Immunohistochemistry

Cryostat sections cut from at least two blocks of each specimen were fixed in a mixture of acetone/methanol (1:1) at $-20\,^{\circ}C$ for 15 min. They were washed with 0.05 M Tris-HCl buffered saline pH 7.6 (TBS), and stained with the biotin streptavidin alkaline phosphatase technique. The sections were exposed to primary antibodies for 16–18 h at $4\,^{\circ}C$. Monoclonal antibodies, RFD1, RFD7 and RFD9 were diluted 1/20, all other antibodies were used at a dilution of 1/100. This was followed by 1 h incubation with biotinylated horse anti mouse IgG antibody. Biotinylated horse anti mouse IgM was used with slides stained with RFD1, and biotinylated goat anti rabbit with those stained for IL-1β. Alkaline phosphatase streptavidin conjugate was added to all slides for 1 h incubation. All conjugated antibodies were purchased from Vector Laboratories, Peterborough, UK, and were used at 1/100 dilution. Each incubation was followed by three washes with TBS for 5 min each. The substrate reaction was developed using 5 mg Naphthol AS-BI phosphate (Sigma) dissolved in 200 µl dimethyl-formamide. This was mixed with 10 ml of 0.1 M Tris-HCl buffer pH 8.2, and 10 mg Fast Red TR salt (Sigma). Levamisole was added at a final concentration of 10^{-3} M as an inhibitor of endogenous alkaline phosphatase. The substrate solution was filtered and used immediately. Sections were then washed and counterstained with Mayers haematoxylin and mounted in glycerine jelly (Dako) or Aquamount (BDH).

The following controls were used to confirm the specificity of the immunostaining: (1) replacing the primary antibody with TBS or non-immune immunoglobulin from the same species as the first antibody, (2) the development of alkaline phosphatase alone to exclude the detection of endogenous alkaline phosphatase in endothelial cells.

2.5. Assessment of the proportion of Mϕ subsets and T cells

To determine the relative frequency of Mϕ subsets and T cells, consecutive sections from each sample were labelled with the antibodies in the following order: CD68, RFD1, RFD7, CD11b, RFD9, CD13, IL-1β and CD3. The average number of positive cells labelled with each of the MAb RFD1, RFD7, RFD9 or anti CD3 was estimated by counting cells in ten representative fields (a minimum of 500 cells). The proportion of $RFD1^+$ or $RFD7^+$ subset was expressed as a percentage of $CD68^+$ Mϕ counted in parallel fields in serial sections. The number of $RFD9^+$ FBGC was assessed as a percentage of the total number of FBGC estimated in each field within the same section. Likewise the percentage of $CD3^+$ cells was determined within the same section as a percentage of the total number of the inflammatory infiltrate present within each particular field. Statistical analysis was performed with the unpaired two-tailed t-test, values of $p < 0.05$ were considered as significant.

2.6. Immunofluorescence double labelling

The indirect and the biotin streptavidin methods were used for the simultaneous localization of two antigens. The sections were fixed in cold acetone for 10 min before staining.

2.6.1. Dual localization of IL-1β (FITC) and RFD7 (Texas Red)

A combination of RFD7 (mouse MAb), 1/10 and IL-1β (rabbit antibody), 1/50 were added together for 1 h incubation, followed after washing in PBS by biotinylated horse anti mouse IgG at 1/100 dilution for 30 min. The sections were then washed in PBS and incubated for 30 min in a mixture of streptavidin Texas Red 1/200 (Vector Laboratories) and FITC conjugated goat anti rabbit IgG, 1/50 (Dako).

All sections were washed in PBS after each incubation, and were finally mounted in citifluor (Citifluor UK Chem Laboratories) and viewed with a Zeiss microscope with selective filters for FITC and TRITC/Texas Red.

3. Results

3.1. Histological assessment

The bone–implant interface obtained from revision of failed TJR showed a prominent Mϕ infiltrate and a variable number of T cells which were mostly perivascular. Fused forms of Mϕ (macrophage polykaryons/foreign body giant cells (FBGC)) showed marked variation in the frequency, size and location within the sections. As Mϕ and their subsets predominate in these tissues, staining for CD68 and CD11b

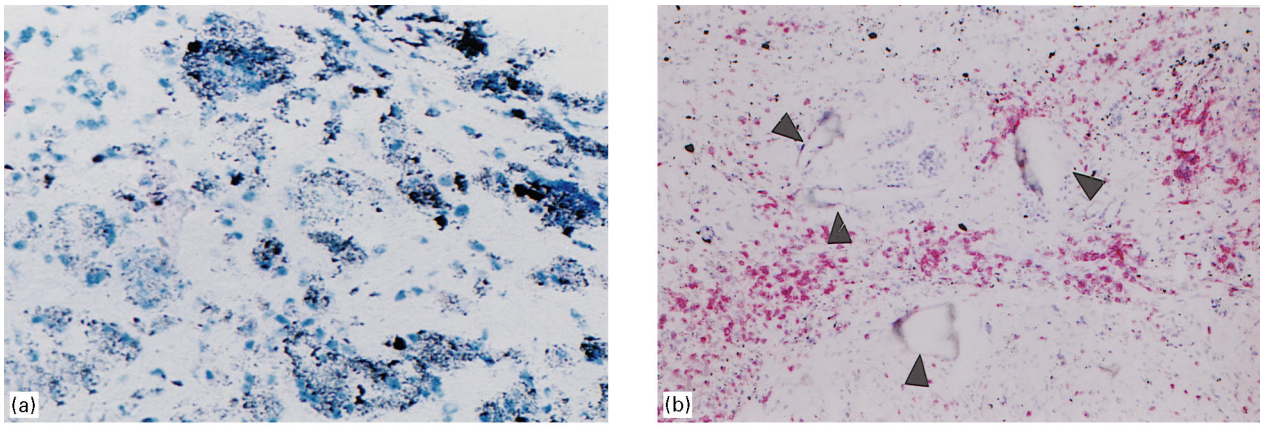

Figure 1 Section of the bone–implant interface membrane from case 4: (a) shows heavy Mϕ infiltrate and FBGC with phagocytosed metal particles; (b). Demonstrates substantial increase in the number of T cells in association with the presence of metal (fine black particles) and large flakes of polyethylene (arrow head).

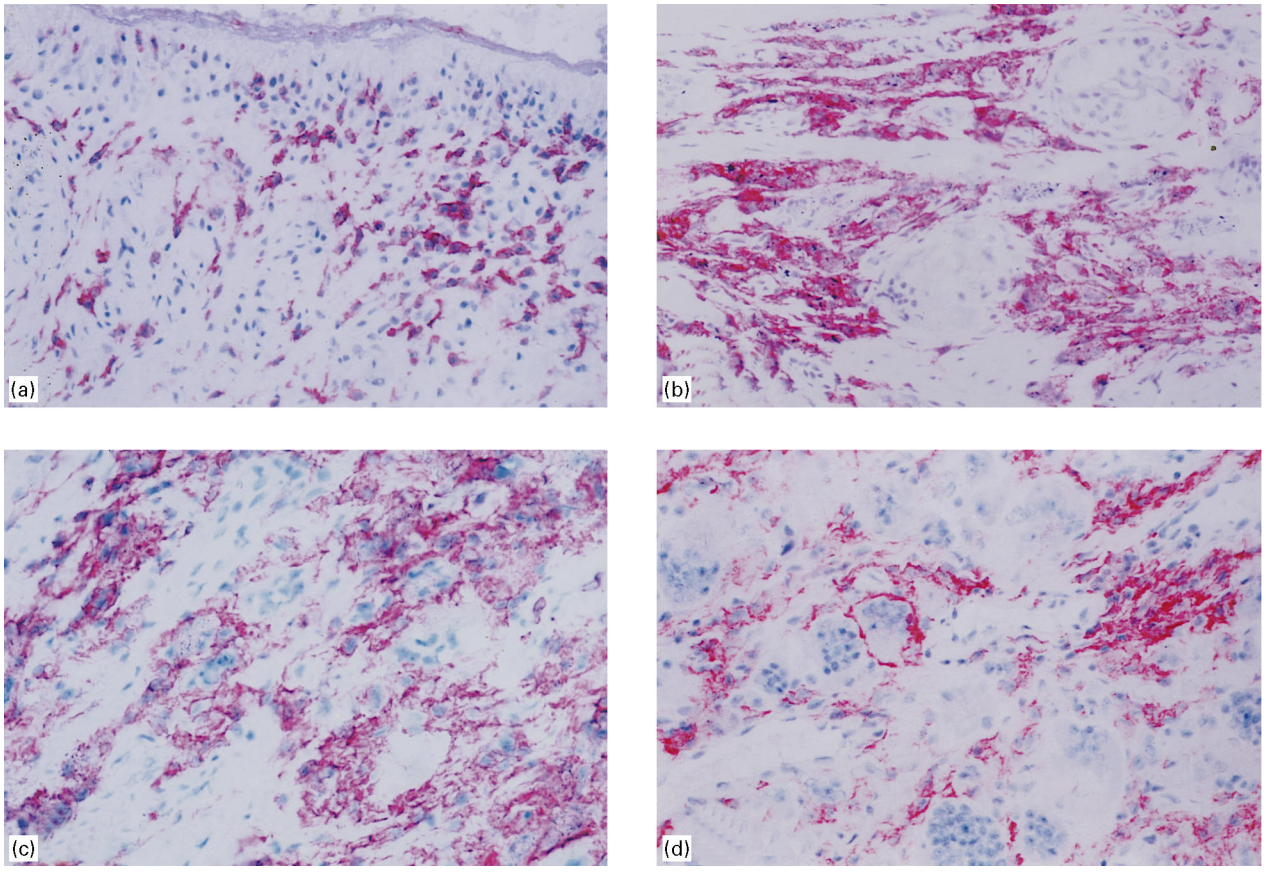

Figure 2 Immunostaining with the MAb RFD1 to illustrate its reactivity in various cases. (a) Rheumatoid arthritis synovium. Positively stained cells have a dendritic-like morphology but show no distinct distribution within the synovial lining or the deeper layers. (b) Section from case 3. Up-regulated expression of RFD1 on different forms of Mϕ including histiocytic and dendritic. (c) Section from case 6 shows marked expansion in the RFD1 + phenotype which included a proportion of the FBGC. (d) Membrane expression of RFD1 on FBGC is clearly demonstrated in this section from case 4.

highlighted the histological pattern of the cellular infiltrate. FBGC were characterized by their strong immunoreactivity with the MAb CD13. Although some of these cells showed irregularly arranged nuclei, a large proportion were of the Langhans (tuberculous) type in which the nuclei had a peripheral location. The increase in the Mϕ infiltrate in these tissues correlated strongly with the presence of high levels of detectable wear particles of metal or PE (Fig. 1a). The pattern of tissue distribution of T cells was almost consistent within the interface membranes analysed. Selective accumulation of T cells was apparent at the perivascular areas and in association with debris containing Mϕ (Fig. 1b). The number of T cells ($CD3^+$) was significantly increased (up to ten-fold) in cases with metal debris.

3.2. Characterization of the Mϕ functional subsets

The reactivity of the MAb RFD1, RFD7 and RFD9 with different forms of Mϕ and the percentage of positive cells in the bone–implant interface are summarized in Table II.

3.2.1. RFD1

The frequency of positive cells for RFD1 MAb varied remarkably between the different groups analysed. No expression for RFD1 was observed in the synovial tissue with normal histology. In OA synovia, $RFD1^+$ cells did not exceed 10% of the total Mϕ population. Immunoreactive cells were mainly perivascular dendritic macrophages. None of these four cases showed histological evidence of inflammatory changes. The $RFD1^+$ phenotype in RA synovia ranged from 30%–50% (Fig. 2a). Dendritic cells constituted the majority followed by a small proportion of tissue Mϕ.The lining layer of the bone–implant interface gave a comparable staining pattern to that seen in RA synovia. $RFD1^+$ dendritic Mϕ formed a dense cellular infiltrate around the small vessels frequently found in these areas. However, there was a statistically significant difference (p 0.0001) in the mean percentage of RFD1 + Mϕ subsets in cases with excessive metal wear debris versus those with PE wear particles. Six cases (cases 3, 4, 6, 10, 14 and 15) showed marked increase in the proportion of the $RFD1^+$ subset (mean percentage 80%, range 60%–90%), (Fig. 2b–d). In addition a high level of membrane expression of RFD1 was evident on the majority of the FBGC in five of these cases (Fig. 2d). A common feature in these samples was the presence of excessive amounts of fine metal particles which were detected within the cytoplasm of the phagocytic Mϕ and FBGC. In comparison the mean percentage of RFD1 + Mϕ in cases with PE only was 30%, range 0%–50%. This considerable increase in the $RFD1^+$ antigen-presenting Mϕ was more frequently observed in the interface tissues obtained from patients whose original joint disease was RA, as indicated in Table II. Exposure to PE particles only (in cases lacking metal debris) in the interface membranes obtained from other RA patients (cases 2 and 5) did not induce a significant elevation in the proportion of $RFD1^+$ subset.

3.2.2. RFD7

RFD7 was expressed at low levels on tissue Mϕ in both normal and OA synovia as indicated by weak membrane staining on these cells. Immunoreactive cells were distributed evenly throughout the section. In RA synovia and periprosthetic tissues, high intensity of staining was observed. Most of the $RFD7^+$ populations in the lining and deeper layers in both conditions had histiocytic morphology. Immunoreactivity for RFD7 was also observed on a proportion of the dendritic Mϕ in the lining layer and the perivascular infiltrate (Fig. 3).

3.2.3. RFD9

Considerable variation in the frequency of $RFD9^+$ cells was observed among the different groups analysed. Immunoreactivity for RFD9 was almost completely restricted to fused Mϕ/FBGC regardless of their location (Fig. 4a). No staining for RFD9 was obtained in normal or OA synovia due to the absence of this cell type. In RA synovia, small aggregates of fused Mϕ (2–5 nuclei) in the lining layer, and the deeper layer of the synovial stroma, demonstrated

TABLE II Reactivity of the monoclonal antibodies to Mϕ functional subsets in the bone–implant interface membrane

Case	Underlying joint disease	Percentage (%) and type of positive cells[a]			Type of debris detected in the section
		RFD1	RFD7	RFD9[b]	
1.	RA	50 (D)	60 (D, H)	80	PE
2.	RA	20 (D, H)	40 (D, H)	0	PE
3.	RA	90 (D, H,FBGC)	80 (D, H)	80	Metal, PE
4.	RA	85 (D, H, FBGC)	80 (D, H)	40	Metal, PE
5.	RA	40 (D, H)	70 (D, H)	60	PE
6.	RA	90 (D, H, FBGC)	75 (D, H)	15	Metal
7.	Sec OA/CDH	40 (D, H)	60 (D, H)	80	PE
8.	OA	30 (D, H)	50 (D, H)	70	PE
9.	Sec OA/CDH	30 (D, H)	50 (D, H)	0	PE
10.	OA	75 (D, H, FBGC)	60 (D, H)	30	Metal
11.	OA	20 (D, H)	50 (D, H)	80	PE
12.	OA	—	50 (D, H)	0	PE
13.	Sec OA/PT	30 (D, H)	50 (D, H)	0	PE
14.	OA	80 (D, H)	75 (D, H)	60	Metal, PE
15.	Sec OA	60 (D, H)	70 (D, H)	90	Metal, PE
16.	OA	35 (D, H)	70 (D, H)	60	PE
17.	OA	35 (D,H,FBGC)	65 (D, H)	70	PE

[a] PE, polyethylene visualized under polarization light; D, dendritic Mϕ; H, histiocytic Mϕ; FBGC, foreign body giant cells; O, no foreign body giant cells in the section; RA, rheumatoid arthritis; OA, osteoarthritis; SecOA/CDH, secondary osteoarthritis as a consequence of congenital dysplasia of the hip; PT, post traumatic.

[b] Calculated as % of total FBGC and not total Mϕ in the section.

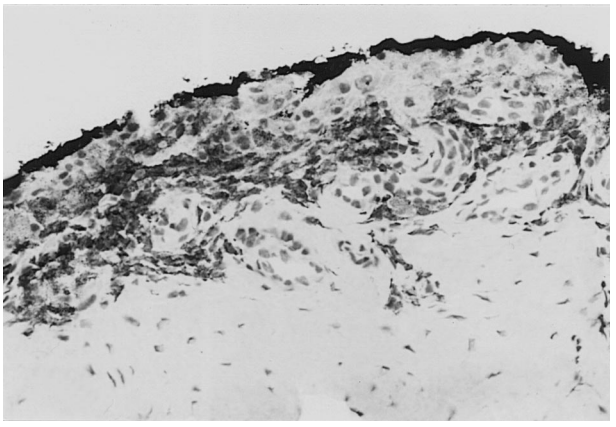

Figure 3 Immunoreactivity of the MAb RFD7 with Mϕ subsets. Sections from case 13. The Mϕ infiltrate is confined to the lining layer only (black indian ink marks the surface of the interface on the implant side).

a high density of membrane and cytoplasmic staining. No other cells in these cases expressed RFD9. Different from the RA synovia, the bone–implant interface membranes were characterized by gradual and consistent transformation of Mϕ subsets into FBGC. FBGC in the lining layer (the implant side) of these tissues resembled those described in RA synovia in terms of their size and staining pattern, although they showed significantly higher frequency. FBGC in the sublining layers and the bone side of the interface were noticeably larger (6–30 nuclei) and showed variation in the frequency of RFD9 expression as shown in Table II. Consistent membrane expression of RFD9 was observed in the vast majority of FBGC in all cases under study. However in three cases (cases 4, 6, 10), large FBGC (containing more than 20 nuclei, and with rather different features from the smaller Langhans-type giant cells) showed reduced/downregulated expression of RFD9. These cases showed reciprocal expression of the two antigens RFD9 and RFD1, the lack of expression of RFD9 on the FBGC being accompanied by high level of RFD1 expression on the same cells. Cell surface expression of RFD9 was also evident on a proportion of multinucleated cells lining the fibrocartilage tissue or mineralized bone on the bone side of the interface (Fig. 4b).

3.3. IL-1 production

IL-1β was demonstrated in the bone–implant interface membranes in eight cases. Six were OA patients (cases 8, 10 and 12–15), the other two had RA (cases 5 and 6). The frequency of IL-1β producing cells varied between these cases. The highest percentage (80%) was found in cases 5, 6, 8 and 15. Both cytoplasmic and membrane bound IL-1β were detected by immunostaining (Fig. 5). Immunofluorescence double labelling indicated that the majority of IL-1β producing cells were $RFD7^+$ tissue macrophages, particularly those within the perivascular infiltrate or in the lining layer. Small numbers of FBGC expressed the membrane form of this cytokine in association with the presence of IL-1β positive Mϕ.

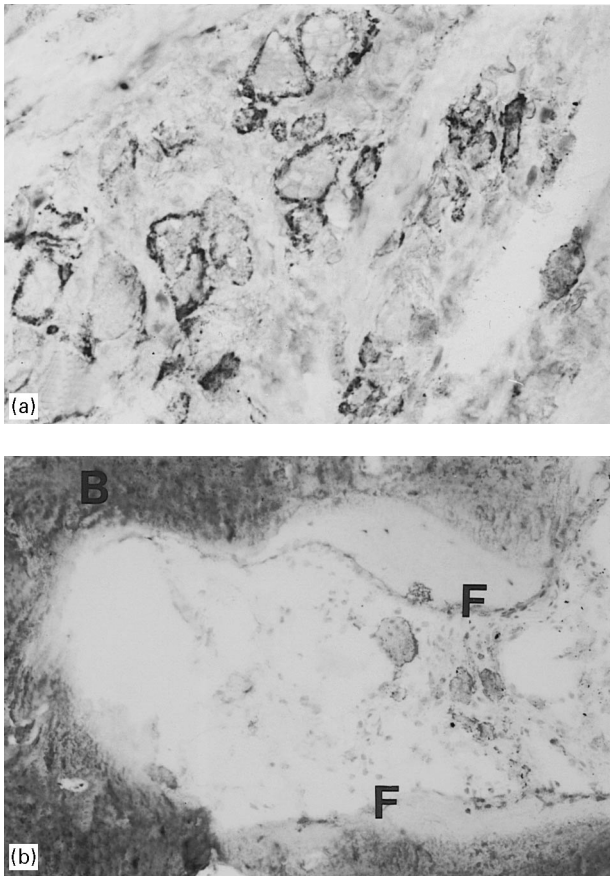

Figure 4 RFD9 expression in the bone–implant interface from case 15. (a) Immunoreactivity of this antibody was mostly restricted to FBGC. (b) Positive staining for RFD9 was also observed on OC/OC-like multinucleated cells lining the fibrocartilage tissue (F) or bone surfaces (B).

4. Discussion

Our results highlight the presence of three distinct functional subsets of Mϕ in the bone–implant interface membranes from patients with inflammatory responses to particulate material from orthopaedic implants. These subsets exhibit morphological, immunophenotypic, and functional differences. This study also demonstrates a significant increase in antigen-presenting phenotype in the interface membrane from patients with metal implants. This significant increase was associated with histological changes consistent with granuloma formation and persistent local chronic inflammatory immune response.

RFD1 identifies an epitope that is HLA-DR linked. The capacity of this antibody to abrogate interactions between T cells and their accessory cells, as demonstrated previously [17], supports the evidence of the role of this molecule in antigen-presentation. Different from diseased rheumatoid synovia in which dendritic cells are the principal antigen-presenting cells (APC) [20], the bone–implant interface membranes demonstrated an expansion of this phenotype to a larger proportion of dendritic Mϕ and histiocytes. In addition, FBGC expressed abundant RFD1 in cases with excessive metallosis (metal deposition in the tissues). It is not clear what role RFD1 expression might have in the cellular transformation of phagocytic Mϕ and the development of erosive lesion within the bone.

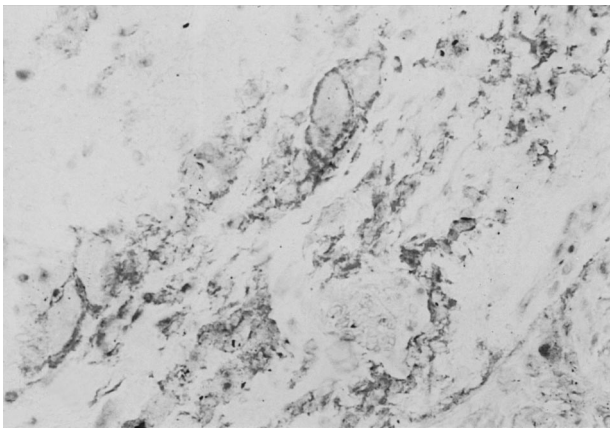

Figure 5 IL-1β production by histiocytic Mϕ in the interface from case 15. Membrane staining for IL-1β was also observed on some FBGC.

Substantial increase in the expression of $RFD1^+$ phenotype on macrophage subsets has been previously demonstrated in other pathological conditions linked to cell-mediated immune/inflammatory responses. Among these are extrinsic allergic alveolitis [21], atopic dermatitis lesions [22], pulmonary sarcoidosis [23] and cutaneous lesions of tuberculoid and leprosy [24]. Consistent with these findings, our observation suggests that the cellular responses elicited by bio-material particles could be antigen-specific immune processes.. The increase in the proportion of RFD1 + Mϕ subset may also account for the selective and enhanced recruitment of distinct T cell subsets to these sites. In our previous report [25] and the present study, a significant increase (up to ten-fold) in the number of T cells was noted in cases with a high level of metal wear particles in comparison to those with polyethylene. Most of these T cells, as we have demonstrated are predominantly CD4 +, CD45RO +, a phenotype of memory primed T cells. On the basis of the extensive expression of RFD1 on metal-containing Mϕ and FBGC and the increased number of perivascular T cells at these sites, a potential interaction between these cells appears to be likely.

Our findings also raise an important question regarding the nature of the processing and presentation pathways of such indegradable particles and the mechanism of interaction between T cells and biomaterial particle-containing phagocytes. In the context of the exposure to metal particles/ions, recent evidence from *in vitro* work has identified different aspects of the modulatory effect of metal exposure on immune-cell function. Exposure to high concentrations of metal particles is thought to be associated with differential activation and the expansion of distinct T cell subsets [26, 27]. Other reports indicate that heavy metals can directly induce increased cytokine production including IL-1 and TNF-α [28, 29] and more important IL-4 by T cells and mast cells [30, 31]. Finally, previous data point to a third mechanism by which metal can augment immune reactivity through local activation of endothelial cells and the up-regulation of cell-adhesion molecules [32]. Such up-regulated expression is known to participate significantly in the process of transvascular migration of the inflammatory infiltrate. These examples, taken together with the observations presented in this study, demonstrate that persistent exposure of cells to high concentrations of metal could have profound effects on the functional capacity of immune cells. However, in view of the signal requirement for effective T cell activation, it has yet to be determined whether metal exposure could enhance the expression of costimulatory signal on antigen-presenting cells and T cells. Indeed further studies within our group are in progress to assess the frequency and the level of expression of the costimulatory molecules B7-1 (CD80)/ B7-2 (CD86) on wear particle-containing Mϕ and the counterreceptor CD28 on T lymphocytes.

The presence of the majority of RFD7 + Mϕ in the perivascular areas within the interface membranes, and the demonstrated production of IL-1β by this distinct subset of Mϕ may offer an insight into the major factors that trigger the recruitment of and the increase in the inflammatory infiltrate. IL-1 is known to be a potential factor in the activation of endothelial cells and the induction of vascular endothelium adhesion molecules [33]. We and others [34, 35] have demonstrated the up-regulated expression of E-selectin, VCAM-1 and ICAM-1 in these tissues, particularly in association with metal-containing Mϕ. This activation pathway could partly be responsible for the persistent inflammatory reaction around loosened implants. Furthermore, the expression of RFD7 on perivascular Mϕ is consistent with previous reports on the acquisition of this antigen following transformation of monocytes into tissue macrophages [36]. Others have also demonstrated the association of RFD7 expression with the increase in the phagocytic capacity of these cells [18]. The prolonged exposure of the Mϕ infiltrate to abundant quantities of metal or PE particles from various implant components may lead to the activation of this particular subset of Mϕ, and the subsequent release of IL-1β. This was confirmed in this study with immunofluorescence double labelling which demonstrated that $RFD7^+$ Mϕ are the major producers of IL-1β in these tissues.

RFD9 immunoreactivity was confined to multinucleated giant cells. A finding that is consistent with previously reported data on the restricted expression of this antigen on epithelioid and multinucleated giant cells in other chronic inflammatory conditions characterized by granuloma formation such as Crohn's disease, sarcoidosis and leprosy [19, 37].

The observation of the positive labelling for RFD9 on multinucleated cells close to the bone surfaces requires further analysis to assess whether RFD9 could be identified as one of the several differentiation markers that distinguish smaller multinucleated cells from large polykaryons. This is particularly interesting in the context of our finding that large FBGC (> 20 nuclei) in the interface either lack or show reduced level of expression of RFD9 in comparison to their smaller counterparts in the same cases. Reports by our group and others [38, 39] revealed that

a proportion of the FBGC in the interface show some resemblance to osteoclasts in terms of morphology, immunophenotypic characteristics and, more important, their functional capacity to resorb bone. Both reports have described the expression of established markers of osteoclast differentiation by these cells. These include vitronectin receptor [38] and the calcitonin receptor [39]. The expression of RFD9 has been shown to be independent of HLA-DR and is thought to be acquired during differentiation of epithelioid Mϕ and multinucleated giant cells [19]. These findings and the data presented raise some questions about the precise role of the RFD9 molecule in Mϕ fusion and the development of multinucleated cells in several granulomatous lesions and in different pathological conditions. The issue of the development of phenotypic markers of osteoclasts and its relationship to RFD9 expression also needs to be clarified.

In conclusion, the present study reveals the potential immunogenicity of indegradable metal particles within the cytoplasm of phagocytic Mϕ in these tissues. RFD1 expression was clearly upregulated in response to metal. This up-regulation was further augmented in the chronically inflamed joint of patients with rheumatoid arthritis. Finally, Mϕ in the interface appear to have distinct functional capabilities when compared to those in peripheral lymphoid tissues. Dissemination of metal to lymph nodes has been shown to cause structural changes including fibrosis, necrosis, or sinus histiocytosis [6, 7, 11]. These observations indicate that the location of these cells may determine the nature and direction of their differentiation. The presence of phagocytic Mϕ in the interface in close proximity to endosteal bone surfaces or calcified bone seems to play a central role in the development of OC-like giant cells and a distinct model of bone resorption at these sites.

Acknowledgements

This work was supported by the Engineering and Physical Sciences Research Council (EPSRC). We wish to thank the orthopaedic surgeons at the Royal Free Hospital and the Royal London Hospital for their collaboration in providing the bone–implant interface and the synovial membranes used in the study. We are grateful to Miss Lynne Walters for secretarial help.

References

1. J. O. GALANTE, J. LEMONS, M. SPECTOR, P. D. WILSON Jr and T. M. WRIGHT, *J. Orthop. Res.* **9** (1991) 760.
2. U. E. PAZZAGLIA and P. D. BYERS, *J. Bone Joint Surg.* **66** [**B**] (1984) 337.
3. A. BARTOLOZZI and J. BLACK, *Biomaterials* **6** (1985) 2.
4. J. J. JACOBS, A. K. SKIPOR, J. BLACK, R.M. URBAN and J. O. GALANTE, *J. Bone Joint Surg.* **73**[**A**] (1991) 1475.
5. T. W. BAUER, M. SALTARELLI, J. T. McMAHON and A. H. WILDE, *ibid.* **75**[**A**] 1993 106.
6. Y. SHINTO, A. UCHIDA, H. YOSHIKAWA, N. ARAKI, T. KATO and K. ONO, *ibid.* **75**[**B**] (1993) 266.
7. C. P. CASE, V. G. LANGKAMER, C. JAMES, M. R. PALMER, A. J. KEMP, P. F. HEAP and L. SOLOMON, *ibid.* **76**[**B**] (1994) 701.
8. S. SANTAVIRTA, Y. T. KONTTINEN, V. BERGROTH, A. ESKOLA, K. TALLROTH, T. S. LINDHOLM, *ibid.* **72**[**A**] (1990) 252.
9. H. J. AGINS, N. W. ALCOCK, M. BANSAL, E. A. SALVATI, P. D. WILSON Jr, P. M. PELLICCI and P. G. BULLOUGH, *ibid.* **70**[**A**] (1988) 347.
10. S. R. GOLDRING, A. L. SCHILLER, M. ROELKE, C. M. ROURKE, D. A. O'NEILL and W. H. HARRIS, *ibid.* **65**[**A**] (1983) 575.
11. J. ALBORES-SAAVEDRA, F. VUITCH, R. DELGADO, E. WILEY and H. HAGLER, *Amer J. Surg. Path.* **18** (1994) 83.
12. W. J. GILLESPIE, C. M. A. FRAMPTON, R. J. HENDERSON and P. M. RYAN, *J. Bone Joint Surg.* **70**[**B**] (1988) 539.
13. T. VISURI and M. KOSKENVUO, *Orthopaedic* **14** (1991) 137.
14. M. PEOCH, C. MOULIN and B. PASQUIER, *New Engng J. Med.* **335** (1996) 133.
15. N. AL-SAFFAR, H. KHWAJA, Y. KADOYA and P. A. REVELL, *Amer J. Clin. Pathol.* **105** (1996) 628.
16. G. JANOSSY, M. BOFILL, L. W. POULTER, E. RAWLINGS, G. D. BURFORD, C. NAVARRETE, A. ZIEGLER and E. KELEMEN, *J. Immunol.* **136** (1986) 4354.
17. L. W. POULTER, D. A. CAMPBELL, C. MUNRO and G. JANOSSY, *Scand. J. Immunol.* **24** (1986) 351.
18. G JANOSSY, M. BOFILL, L. W. POULTER, in "Immunocytochemistry today" (Wright, Bristol, 1985).
19. C. S. MUNRO, D. A. CAMPBELL, L. A. COLLINGS and L. W. POULTER, *Clin. Exp. Immunol.* **68** (1987) 282.
20. A. C. H. M. VAN DINTHER-JANSSEN, S.T. PALS, R. SCHEPER, F. BREEDVALD and C.J.L.M.MEIJER, *J. Rheumatol.* **17** (1990) 11.
21. M. A. JOHNSON, A. NEMETH, A. CONDEZ, S. W. CLARKE and L. W. POULTER. *Eur. Respir. J.* **2** (1989) 444.
22. V. A. ALEGRE, D. M. MacDONALD, L. W.POULTER *Clin. Exp. Immunol.* **64** (1986) 330.
23. M. A. SPITERI, S. W. CLARKE and L. W. POULTER, *ibid.* **74** (1988) 359.
24. L. A. COLLING, M. F. R. WATERS and L. W. POULTER, *ibid.* **62** (1985) 458.
25. N. AL-SAFFAR and P. A. REVELL, *Br. J. Rheumatol.* **33** (1994) 309.
26. Y. JIANG and G. MOLLER, *J. Immunol.* **154** (1995) 3138.
27. F. SINIGAGLIA, *J. Invest. Dermatol.* **102** (1994) 398.
28. J. M. ZDOLSEK, O. SODER and P. HULMAN, *Immunopharmacol.* **28** (1994) 201.
29. S. LISBY, K. M. MULLER, C. V. JONGENEEL, J. H. SAURAT and C. HAUSER, *Int. Immunol.* **7** (1995) 343.
30. P. PRIGENT, A. SAOUDI, C. PANNETIER, P. GRABER, J.Y. BONNEFOY, P. DRUET and F. HIRSCH. *J. Clin. Invest.* **96** (1995) 1481.
31. D. B. C. OLIVEIRA, K. GILLESPIE, K. WOLFREYS, P. W. MATHIESON, F. QASIM and J. W. COLEMAN, *Eur. J. Immunol.* **25** (1995) 2259.
32. M. GOEBELER, G. MEINARDUS HAGER, J. ROTH, S. GOERDT and C. SORG. *J. Invest. Dermatol.* **100** (1993) 759.
33. M. P. BEVILACQUA, J. S. POBER, D. C. MENDRICK, R. S. COTRAN and M. A. GIMBRONE, *Proc. Nat. Acad. Sci. USA* **84** (1987) 9238.
34. N. AL-SAFFAR, J. T. L. MAH, Y. KADOYA and P. A. REVELL. *Ann. Rheum. Dis.* **54** (1995) 201.
35. C. L. KLEIN, P. NIEDER, M. WAGNER, H. KOHLER, F. BITTINGER, C. J. KIRKPATRICK and J. C. LEWIS, *J. Mater. Sci. Mater. Med.* **5** (1994) 798.
36. N. HOGG, S. MacDONALD, M. SLUSARANKO and P. C. L. BEVERLEY, *Immunology* **53** (1984) 753.
37. M. C. ALLISON and L. W. POULTER, *Clin. Exp. Immunol.* **85** (1991) 504.
38. Y. KADOYA, N. AL-SAFFAR, A. KOBAYASHI and P. A. REVELL, *Bone Mineral.* **27** (1994) 85.
39. S. R. GOLDRING, M. ROELKE and J. GLOWACKI, *J. Bone Min. Res.* **3** (1988) 117.

Received 1 May
and accepted 30 May 1997